JMEPEG (2004) 13:93-98
DOI: 10.1361/10599490417597

1059-9495/$19.00

Crack Propagation Resistance Along Strength Mismatched Bimetallic Interface

F. Jiang, Z.L. Deng, J. Sun, and J.F. Wei

(Submitted 18 October 2002; in revised form 20 October 2003)

Bimetallic three-point-bending specimens and four-point-bending fatigue test specimens were produced from strength mismatched stainless steel/low carbon steel bi-material. Both the *J* resistance curves and fatigue crack growth behavior were investigated for the bi- and bulk materials. The results showed that a crack initiated easily at the interface, and crack growth resistance along interface was inferior to that of the corresponding bulk materials under either static or dynamic loading conditions.

Keywords explosive clad metal, fatigue crack growth, interfacial crack

1. Introduction

Bi-material systems with a strength mismatch are encountered in several engineering applications. Typical examples include solid joints in weldments and explosive-clad metallic bonds in pressure vessels. In many of these situations cracks are initiated at interfaces and advance either along or away from the interface.[1-5] Performance of such systems depends on the failure characteristics of the interfaces. The reliability of such components inevitably requires a thorough understanding of their behavior under loads. The measurement of interfacial strength and toughness and understanding the fatigue crack growth behavior along the bi-material interface was of practical interest.

The fracture toughness of several kinds of bi-material interfaces in terms of the *J* integral have been previously investigated.[1,2] The applicability of the *J* integral approach for property mismatched bi-material systems was verified recently.[2,6-8] For the fatigue crack growth behavior along an interface, many theoretical analyses (both analytical studies and finite element simulations[9-11]) and experimental studies (e.g., in bi-material systems such as ceramic/metal and polymer/metal[12-14]) have been undertaken. However, there have been relatively few research studies[3,15] investigating the fatigue crack growth behavior at the interface of metal/metal bi-materials.

In the present work, bimetallic three-point-bend (TPB) specimens and four-point-bend (FPB) fatigue test specimens were produced from explosively clad stainless steel/low carbon steel (1Cr18Ni9Ti/20G) couples. *J* resistance curves generated from normal TPB and FPB specimens were investigated for the bi-material interface specimens and the bulk material specimens. The crack deviation from an interface was examined.

F. Jiang, Z.L. Deng, J. Sun, and **J.F. Wei,** State Key Laboratory for Mechanical Behavior of Materials School of Materials Science and Engineering, Xi'an Jiaotong University, Xi'an 710049, People's Republic of China. Contact e-mail: junsun@mail.xjtu.edu.cn.

2. Experimental Procedure

Steel-steel bi-material laminates were made by the explosive cladding technique, using stainless steel (1Cr18Ni9Ti) and low carbon steel (20G). The mechanical properties and chemical compositions of two metals can be found in Ref 16. The explosive cladding procedure produced a wavy interface in the laminates. Figure 1 shows the typical profiles of these interfaces. A wavelike configuration along the explosive wave direction is indicated in Fig. 1(a), and a flat one normal to the wavy direction is shown in Fig. 1(b). Similar interface profiles can be found in pure aluminum/alumina alloy 2024 explosively clad plate.[2] According to the method used by Tschegg et al.,[1] $10 \times 16 \times 150$ mm strips from laminates with flat interface profiles were prepared for electron beam welding and blocks of the same metals were electron beam welded to the 1Cr18Ni9Ti and 20G surfaces, respectively. TPB specimens involving bi-material interfaces were cut from these clad-clad plates and notches were introduced at the interface by spark erosion and pre-fatigue cracking. The thickness B was 10 mm and the height W was 20 mm. Initial crack length a_0 was about 10 mm and the a/W ratio was about 0.5. After pre-fatiguing, side grooves were machined to the test specimens along both sides of the interface to make sure the crack grows along the interface leading to plane strain test conditions. The side grooves were machined with an angle of 60° to a depth equal to 10% of the specimen thickness B. The radius of the side groove root was about 0.45 mm with this radius ensuring that the interface was contained in the range of side grooves. The final shape of specimens for TPB testing are shown in Fig. 2(b).

FPB fatigue test specimens involving bi-material interfaces were also cut from these clad-clad plates. The final shape of specimens for fatigue testing is shown in Fig. 2(d).

All bimetallic specimens made of 1Cr18Ni9Ti/20G were heat treated at 860 °C for 2 h and furnace cooled to remove any residual strain hardening induced by explosive cladding.

The specimens of bulk 1Cr18Ni9Ti and 20G for TPB and FPB fatigue testing also were prepared in much the same way. Their sizes, shapes, and heat treatment conditions were the same as those of the bimetallic 1Cr18Ni9Ti/20G specimens. Bulk specimen geometries are illustrated in Fig. 2(a) and 2(c).

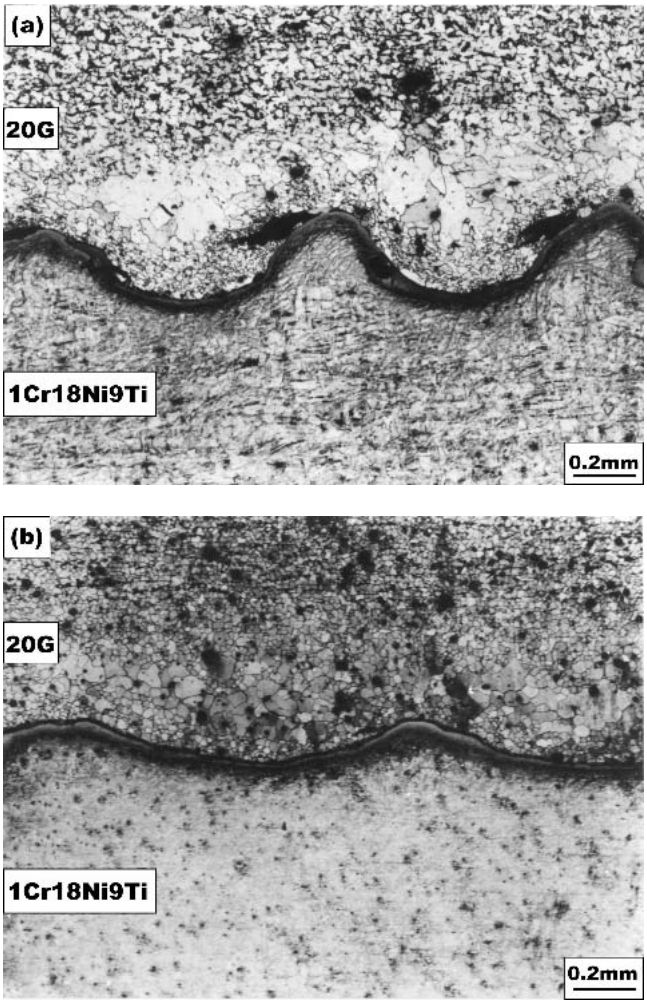

Fig. 1 Interface morphology of 1Cr18Ni9Ti/20G and microstructures of both sides of interface: **(a)** wavy interface and **(b)** flat interface

For TPB test specimens, pre-fatigue cracks were introduced into the interface at the roots of the notches by four-point-bend fatigue for 10^5 cycles at certain ΔK values using an Amsler HFP5100 fatigue-testing machine (Zwick Roell Group, Germany). The details of the measurement of J resistance curves were same as that described in Ref 2, with tests performed on an MTS-880 testing machine (MTS Systems Corporation, Oak Ridge, TN) using a crosshead speed of 0.05 mm/min. While testing, the load-displacement curves (P-δ) were recorded and the corresponding crack length a_i was obtained through the use of a traveling microscope with a precision of 0.01 mm.

All FPB fatigue tests were performed using an Amsler HFP5100 fatigue-testing machine. The amplitude of the applied stress was kept constant at a load ratio (R) of 0.1. The cyclic frequency was about 100 Hz (sinusoidal wave). Crack length was measured using a traveling microscope with a precision of 0.01 mm. At the same time, a direct current electric potential drop method was used as a complementary method to monitor the length of the growing fatigue cracks.

Scanning electron microscopy (SEM) and optical microscopy (OM) were used to observe the fatigue crack profiles and the fracture surface.

3. Results and Discussion

3.1 J-R Curves

The TPB specimens included bi-material 1Cr18Ni9Ti/20G and bulk steels 1Cr18Ni9Ti and 20G. Each J-R curve was obtained from five specimens with the details of measuring J-R curves found in Ref 2. The results are plotted in Fig. 3. The results indicate that the resistance to crack propagation of the bimetallic 1Cr18Ni9Ti/20G interface was inferior to those of the bulk steels. The resistance to crack growth along the two bimetallic interfaces was always lower than those of respective counterpart metals. It should be noted that the inferior crack growth resistance of interface did not mean that the combined strength of interface was always inferior to the bulk steels. In static tensile tests where the bimetallic interface was perpendicular to the loading direction, fracture often took place in the 20G adjacent to, but not along, the interface. The weak resistance to crack propagation along the interface might be related to the following factors. First, the stress and strain concentration and the inconsistent deformation produced by base metal strength mismatch would prompt the initiation and growth of the crack along the interfaces. Second, during the explosive-clad procedure, impurities, voids, and other joining defects will inevitably be located at the interface. These crack-like defects might grow and coalesce during the process of pre-fatigue cracking, which would degrade the interface strength. A well-defined crack had to be introduced on the interface to measure the J-R curve. However, the pre-fatigue process for TPB specimens would weaken the interfacial toughness. A method that could introduce a well-defined crack on the interface and yet not weaken the interfacial toughness needs to be explored.

3.2 Fatigue Crack Growth Behavior

Fatigue crack growth tests were undertaken for both bi-metal and bulk steels. Because 1Cr18Ni9Ti and 20G had the same Young's modulus (E) and stress intensity factor range (ΔK) as the bi-metal samples, FPB fatigue testing was performed using the same procedure in all cases.

Figure 4 shows the variation in fatigue crack growth rate da/dN versus stress intensity factor range ΔK. The da/dN – ΔK curves of fatigue crack along the interface had three regimes, just like the steels: a near threshold regimen, a stable crack growth regimen and a fast crack growth regimen. The results indicated that the fatigue crack threshold ΔK_{th} of the bi-metal couple was inferior to those of bulk steels. The reason that the crack initiated more easily at the interface might be because crack-like defects including impurities, voids and other defects are located at interface. This is inevitable during explosive cladding, and as a result these pre-existing anomalies might grow and coalesce during fatigue testing. The stress and strain concentration and the inconsistent deformation produced by the base metal strength mismatch might also prompt the initiation and growth of cracks along the interface. In the stable growth regimen, under the same stress intensity factor range ΔK, the da/dN along the interface was greater than that in the steels. This means that the fatigue growth resistance along the interface was lower than that in the bulk steels.

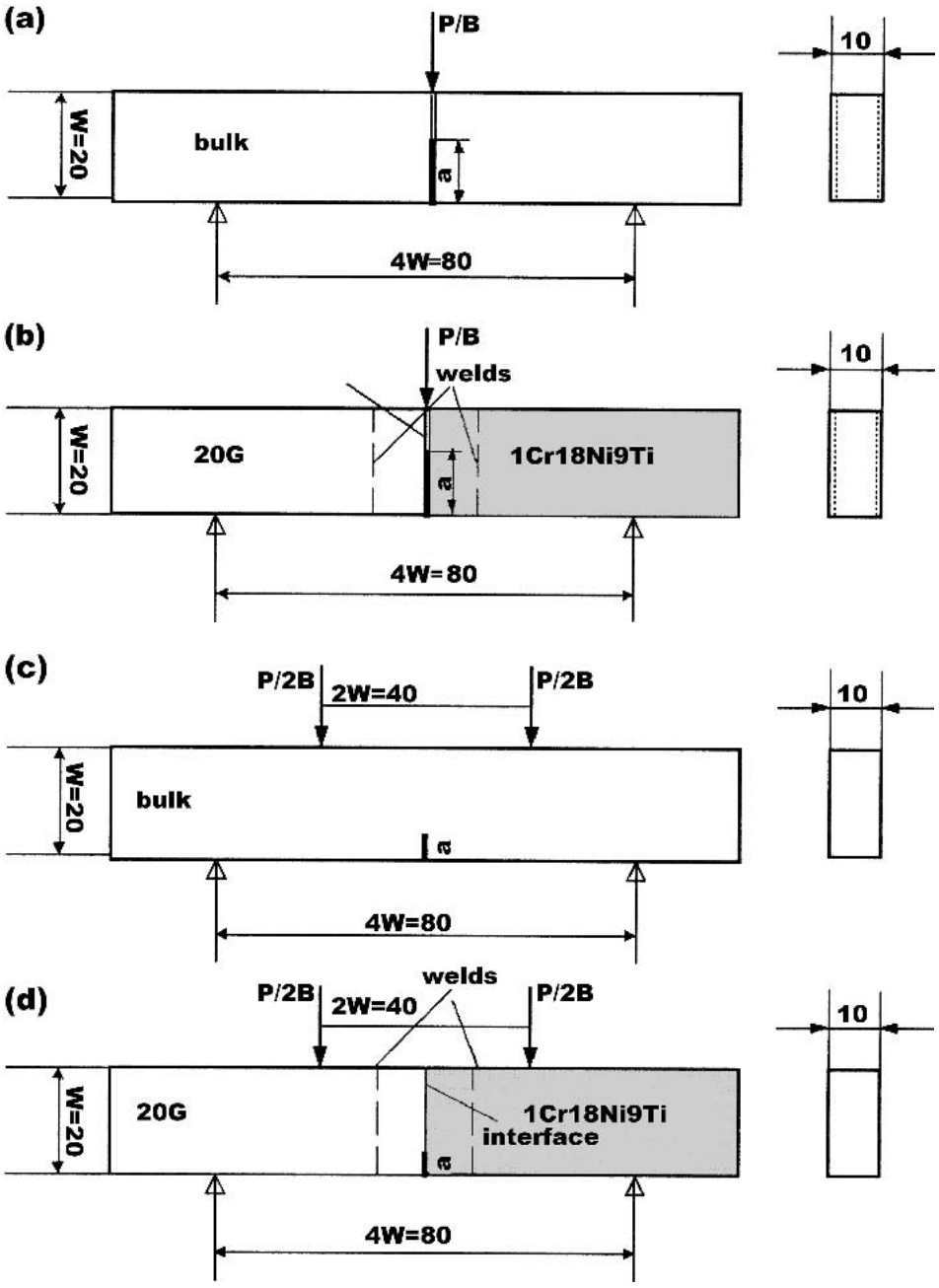

Fig. 2 Schematic representation of specimens used in measuring **(a,b)** *J* and **(c,d)** four-point-bending fatigue

3.3 Fractographic Observation

For the *J-R* curve test, the top view of a fracture surface with side grooves is shown in Fig. 5, in which the mark M indicates the mechanical notch, S indicates the spark-eroded one, and P indicates the pre-crack introduced by pre-fatigue cycling. F indicates the fracture surface of TPB test, and R indicates the final rupture surface. In the present work, without constraint from the side grooves, the interfacial cracks would deviate into 20G, the softer alloy steel in the bi-metal system (see Fig. 6), and the *J-R* curve could not be obtained. Similar results (i.e., a crack growing towards the softer metal) were also found in dissimilar steels[4] and welded joints.[5] In a strength mismatched bi-material system under far field mode *I* conditions, a localized zone of high hydrostatic stress develops near the crack tip but then expends rapidly into the weaker material as the plasticity spreads across the ligament of the specimen.[17] Strain gradient theory analysis also reveals that high stress triaxiality promotes ductile damage and facilitates crack growth. This always occurs on the softer material side.[18] Furthermore, a finite element method simulation[2] showed that in the strength mismatched pure aluminum/alumina (Al/LY12) bi-material system, high stress triaxiality always occurs on the softer pure aluminum side under normal three-point-bending.

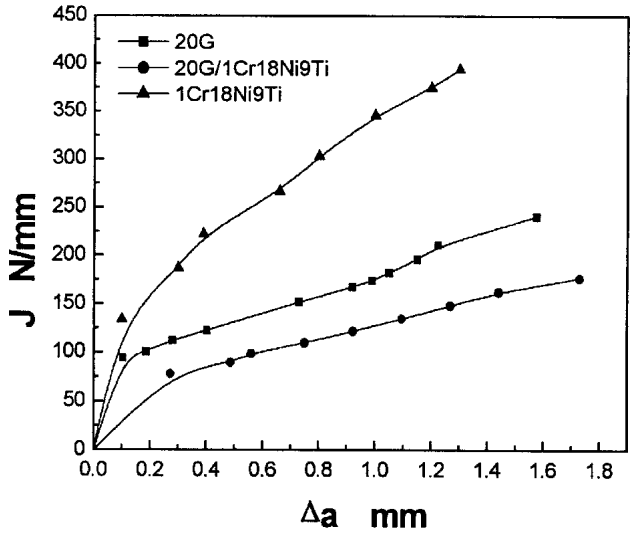

Fig. 3 Crack growth resistance curves of bi-metals and bulk steels

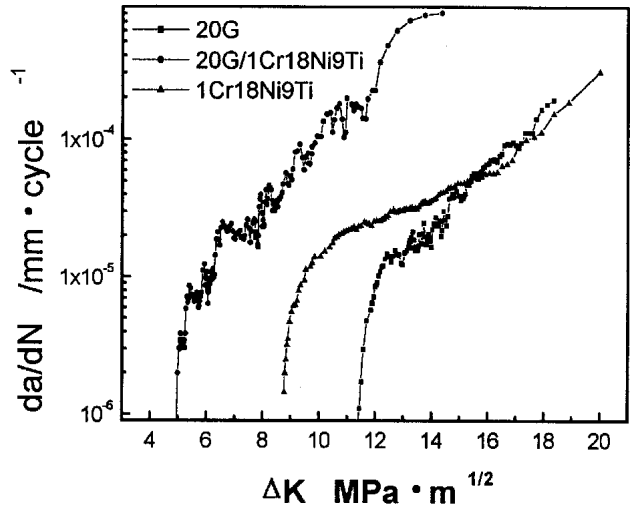

Fig. 4 Crack propagation curves (d*a*/d*N* – Δ*K*) of bi-metals and bulk steels

The existence of high hydrostatic stress and high stress triaxiality in the weaker material under symmetric three-point-bend loading, such as normal three-point bending, implied that an interfacial crack might grow along the interface or deviate into the lower strength metal, but never turned into the higher strength one. Similarly in the 1Cr18Ni9Ti/20G system, high stress triaxiality should deflect the crack from the interface towards the 20G steel side, the lower strength steel in the bi-metal system. Here, side grooves were added along the interface to ensure that the crack grew along interface and the *J-R* curve could be obtained.

The fracture surface of a fatigue tested specimen is shown in Fig. 7. Three distinct regions are seen: M indicates the spark-eroded one, F indicates the fatigue crack propagation surface, and R indicates the surface left by a final rupture. In the fatigue growth regimen, fatigue striations were typically observed (see Fig. 8a). Due to the strength mismatch of the two metals, the

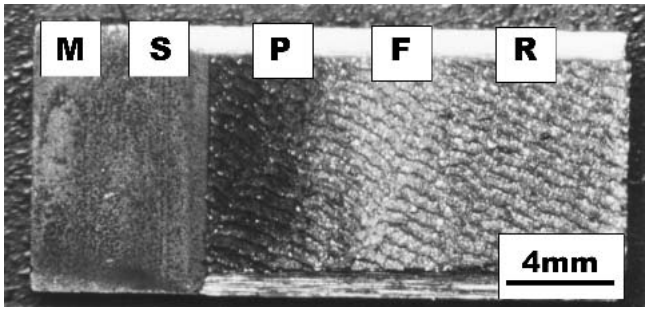

Fig. 5 A fracture surface of three-point-bend specimen. M indicates the mechanical notch. S indicates the spark-eroded one. P indicates the pre-crack introduced by pre-fatigue cycling. F indicates the fracture surface of the TPB test while R indicates the final rupture surface

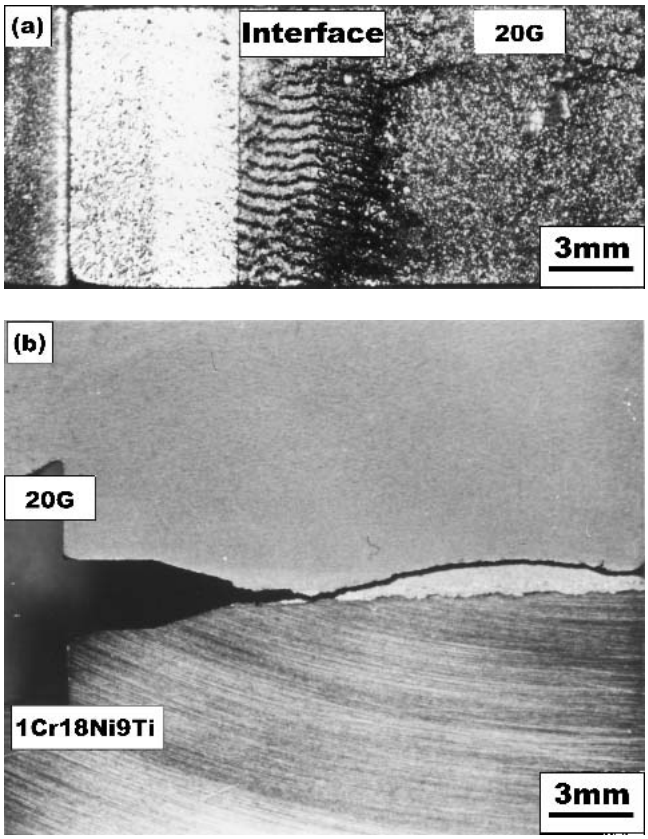

Fig. 6 A crack deviated into weaker material under symmetric three-point-bend loading and plain stress condition: **(a)** fracture surface and **(b)** side view of two specimen halves after rupture

fatigue crack tip was subjected to mixed mode loading under symmetric four-point-bending, leading to a mixed mode condition at the crack tip.[11] The crack planes would contact and some "worn" areas can be seen on the fracture surface (Fig. 8a). Figure 8(b) shows the profile of final rupture surface. Slip lines and elongated dimples are seen on the surface. The elongated dimples were generated due to the mixed mode at the crack tip due to the strength mismatch. Figure 9(a) shows the fatigue crack growth path along the interface while Fig. 9(b) indicates that there were micro-cracks ahead main crack tip.

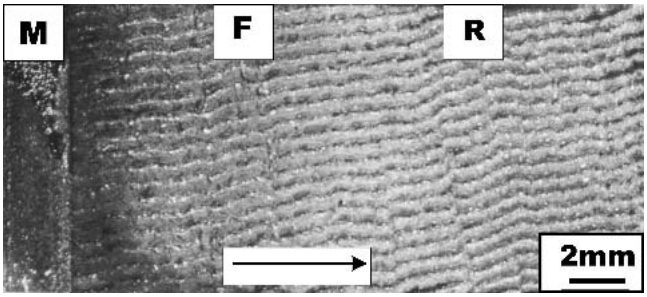

Fig. 7 Fracture surface of fatigue test specimen: M indicates the spark eroded one, F indicates the fatigue crack propagation surface, and R indicates the surface left by final rupture

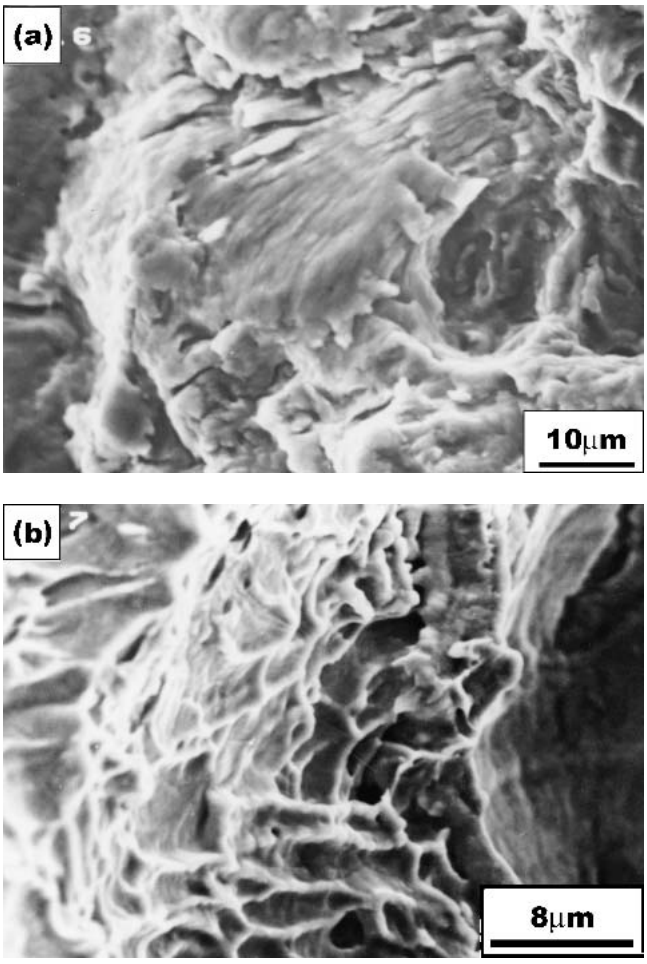

Fig. 8 Scanning electron microscope images of fracture surface showing fatigue striations of **(a)** fatigue zone and **(b)** slip lines and dimples in rupture zone

These micro-cracks might initiate from impurities or debonding of the interface. While undergoing cyclic deformation, the main crack and subsidiary micro-cracks might propagate in the following way: While the main crack tip grows in the forward direction, the micro-crack tip close to main crack might propagate in the opposite direction to the main tip. The tip of the micro-crack away from the main crack tip might, however,

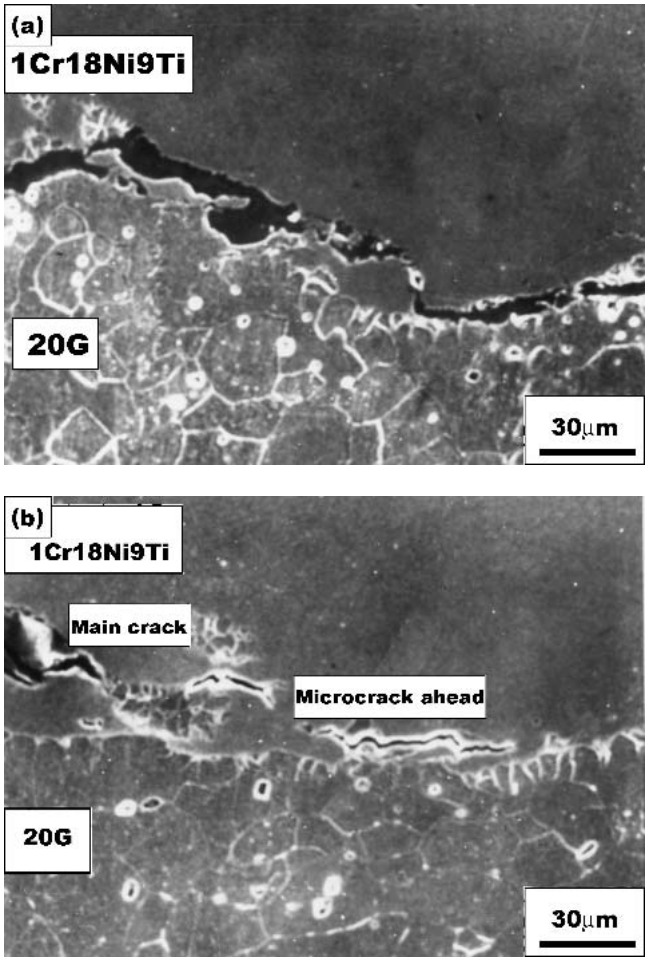

Fig. 9 Scanning electron microscope images of crack propagation: **(a)** the fatigue crack growth path and **(b)** main crack and micro-cracks ahead the main crack tips

propagate in the same direction as the main crack tip. The differential movement of the main crack and micro-cracks were also found to occur in the Al/Al_2O_3 interface[19] and Au/Al_2O_3 interface.[20] At some point, the main crack and micro-cracks would join together during final static fracture. The process of main crack and micro-cracks propagating and joining later could be repeated many times. Because the size of interfacial micro-cracks (>20 μm) was larger than those found in the steel, the joining of the main crack with the micro-cracks would affect the measured crack growth rate da/dN (i.e., the $da/dN - \Delta K$ curve for the bi-metal system fluctuated somewhat).

4. Conclusion

Both the J resistance curves generated during symmetric three-point bending and during cyclic deformation during symmetric four-point bending were investigated using strength mismatched bimetal 1Cr18Ni9Ti/20G couples and their counterpart bulk steels. The results showed that cracks initiated easily at the interface and crack growth resistance along the interface was inferior to that of the corresponding bulk steels under both static and dynamic loading conditions.

Acknowledgments

Financial support from the National Natural Science Foundation of China is gratefully acknowledged. One of the authors, Jun Sun, wishes to express his special thanks for the support of the National Outstanding Young Investigator Grant of China.

References

1. E.K. Tschegg, H.O.K. Kirchner, and M. Kocak: "Cracks at the Ferrite-Austenite Interface," *Acta Metall.,* 1990, *38*(3), pp. 469-78.
2. F. Jiang, K. Zhao, and J. Sun: "Evaluation of Interfacial Crack Growth in Bimaterial Metallic Joints Loaded by Symmetric Three-Point Bending," *Int. J. Pressure Vessel Piping, 80*(2), 2003, pp. 129-37.
3. K. Ohj, Y. Nakai, and S. Hashimoto: "Strength of Interface in Stainless Clad Steels," *Zairyo/J. Soc. Mater. Sci., Jpn.,* 1990, *39*(439), pp. 375-81.
4. R.J. Asaro, N.P. O'Dowd, and C.F. Shih: "Elastic-Plastic Analysis of Cracks on Bimaterial Interfaces: Interfaces With Structure," *Mater. Sci. Eng. A,* 1993, *162,* pp. 175-92.
5. A.C. Bannister, "Fracture Behavior of Mismatched Welded Joints in a Quenched and Tempered Steel of 800 MPa Yield Stress" in Mismatching of Interfaces and Welds, K.H. Schwalbe and M. Kocak, ed., GKSS Research Center, Geesthacht, Germany, 1997.
6. Y.J. Kim, K.H. Schwalbe, and R.A. Ainsworth: "Simplified *J*-estimations Based on the Engineering Treatment Model for Homogeneous and Mismatched Structures," *Eng. Fracture Mech.,* 2001, *68,* pp. 9-27.
7. H. Lee: "Estimation of Crack Driving Forces on Strength-Mismatched Bimaterial Interfaces," *Nucl. Eng. Design,* 2002, *212,* pp. 155-64.
8. Y.J. Kim: "Experimental J Estimation Equations for Single-Edge-Cracked Bars in Four-Point Bend: Homogeneous and Bi-Material Specimens," *Eng. Fracture Mech.,* 2002, *69,* pp. 793-811.
9. X.P. Xu and A. Needleman: "Numerical Simulations of Dynamic Crack Growth Along an Interface," *Int. J. Fract*., 1996, *74,* pp. 289-324.
10. X.P. Xu and A. Needleman: "Numerical Simulations of Dynamic Interfacial Crack Growth Allowing for Crack Growth Away From the Bond Line," *Int. J. Fract.,* 1995, *74,* pp. 253-75.
11. C. Woeltjen, C.F. Shih, and S. Suresh: "Cyclic Near-Tip Fields for Fatigue Cracks Along Metal-Metal and Metal-Ceramic Interfaces," *Acta Metall. Mater.,* 1993, *41*(8), pp. 2317-35.
12. R.M. Cannon, B.J. Dalgleish, R.H. Dauskardt, T.S. Ohj, and R.O. Ritchie: "Cyclic Fatigue-Crack Propagation Along Ceramic/Metal Interfaces," *Acta Metall. Mater.,* 1991, *39*(9), pp. 2145-56.
13. D.R. Bloyer, K.T. Venktateswara Rao, and R.O. Ritchie: "Laminated Nb/Nb_3Al Composites: Effect of Layer Thickness on Fatigue and Fracture Behavior," *Mater. Sci. Eng. A*, 1997, *239,* pp. 393-98.
14. Z.H. Zhang and J.K. Shang: "Subcritical Crack Growth at Bimaterial Interfaces: Part III. Shear-Enhanced Fatigue Cracks Growth Resistance at Polymer/Metal Interface," *Metall. Mater. Trans. A*, 1996, *27,* pp. 221-28.
15. H. Nayeb-Hashemi and P.H. Yang, "Mixed Mode I/II Ffracture and Fatigue Crack Growth Along 63Sn-37Pb Solder/Brass Interface," *Int. J. Fatigue,* 2001, *71,* pp. s325-35.
16. F. Jiang, Z.L. Deng, and J. Sun: "Fatigue Crack Propagation Normal to a Plasticity Mismatched Bimaterial Interface," *Mater. Sci. Eng. A,* 2003, *356*(1-2), pp. 258-66.
17. C.F. Shih, R.J. Asaro, and N.P. O'Dowd: "Elastic-Plastic Analysis of Cracks on Bimaterial Interfaces. Part III. Large-Scale Yielding," *J. Appl. Mech. Trans. ASME* 1991, *58,* pp. 450-63.
18. S. Hao and W.K. Liu: "Bimaterial Interfacial Crack Growth With Strain Gradient Theory," *J. Eng. Mater. Technol.,* 1999, *121,* pp. 413-21.
19. A.G. Evans and B.J. Dalgleish: "Fracture Resistance of Metal-Ceramic Interfaces," *Acta Metall. Mater.,* 1992, *40,* pp. s295-306.
20. M.R. Turner and A.G. Evans: "Experimental Study of the Mechanisms of Crack Extension Along an Oxide/Metal Interface," *Acta Mater.,* 1996, *44*(3), pp. 863-71.